Original

Measurement of Modulation Transfer Functions for Liquid Crystal Displays by Rectangular Waveform Analysis

AKIKO HORII, AYA CHIHARA,[1)] KATSUHIRO ICHIKAWA,[2)] YOSHIE KODERA,[2)] MITSURU IKEDA,[2)] and TAKEO ISHIGAKI

Graduate School of Medical Sciences, Nagoya University
1)Department of Radiology, Saishunso National Hospital
2)School of Health Sciences, Nagoya University

Received July 11, 2005
Revision accepted Nov. 1, 2005
Code No. 522

Introduction

In current medical imaging diagnosis, new diagnostic techniques using image viewers equipped with a cathode ray tube (CRT) display or liquid crystal display (LCD) have replaced the conventional film-based diagnostic techniques. It can be expected that this trend will continue to increase in the future. With this change, it is becoming important to evaluate the characteristics of displays and to carry out maintenance management in medical facilities that use CRT displays and LCDs. Therefore, as one form of determining the image quality of a display, modulation transfer function (MTF) is measured by evaluating sharpness.

The method we used is based on a periodic rectangle wave composition of fundamental frequency and harmonics that are sine waves.[1)] The flow of this method is shown in Fig. 1. The profile of a direction perpendicular to the bar of the bar patterns was created from image data and converted into the brightness value. The component value of a fundamental frequency, Mn (n: segment number), was calculated from exact integer cycle data extracted from the interpolated profile data. In was calculated from the bar pattern and the background levels measured from two uniform areas. The ratio of Mn to In was calculated for MTF.

This was the method of calculating MTF in the horizontal direction of CRT display. The LCDs are discrete display systems and are composed of individual pixels. Therefore, it is necessary to correct the results of the calculation method for the CRT display system (analog system). We multiplied MTFs by the correction factor, except for those in the horizontal direction of the CRT display.

1. Methods

1-1 Display of bar pattern

We used LCDs of 1M (about 1 million pixels), 2M, 3M, and 5M, and a CRT display with a pixel number of 5M. The table shows the specifications of displays. For

Summary

We measured modulation transfer functions (MTFs) of liquid crystal displays (LCDs) by rectangular waveform analysis. This method consists of taking a picture of the bar pattern on the display surface with a digital camera, and analyzing the picture with a personal computer. The displays used are LCDs of 1M (about 1 million pixels), 2M, 3M, and 5M, and a cathode ray tube (CRT) display with a pixel number of 5M. Two kinds of 2M displays were used, an in-plane switching (IPS) system and vertical alignment (VA) system, from which liquid crystal operation mode differs. MTFs increased as pixels increased. For the LCDs, MTFs in the horizontal direction were higher than those in the vertical direction except for the 2M VA system. For the LCD of the 2M VA system, MTF in a horizontal direction was equal to MTF in a vertical direction. For the displays with the same number of pixels (5M), MTF of a LCD was higher than that of a CRT display. MTFs of LCDs are influenced by the pixel form, pixel composition, and the liquid crystal operation mode.

Key words: *Liquid crystal display (LCD), Cathode ray tube (CRT) display, Modulation transfer function*

別刷資料請求先：〒461-8673 愛知県名古屋市東区大幸南1丁目1番20号
名古屋大学大学院医学系研究科 堀井亜希子 宛

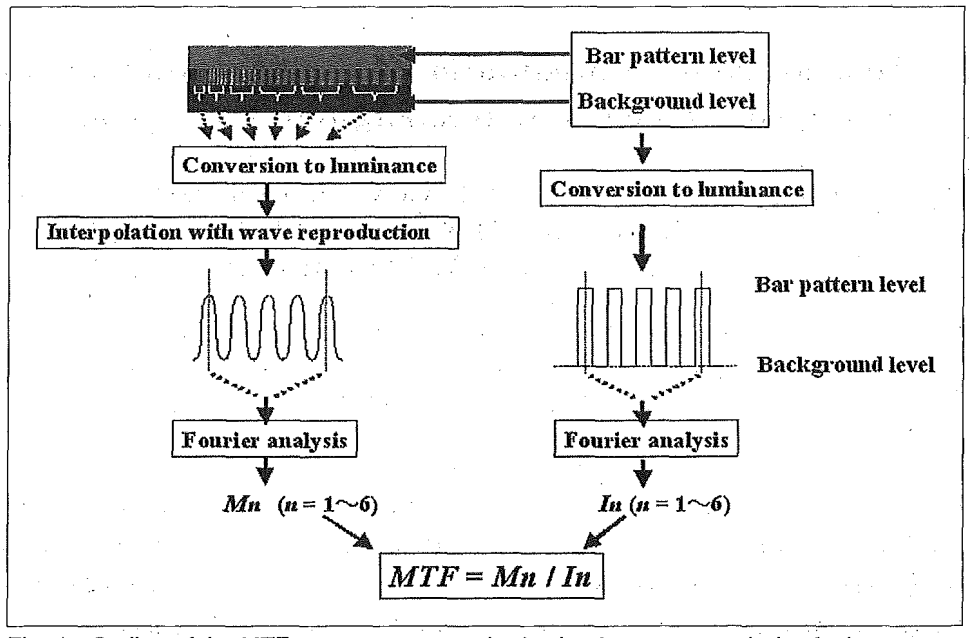

Fig. 1 Outline of the MTF measurement method using frequency analysis of a bar pattern image.

Table Specifications of displays used in this study.

	Pixel size	Pixel pitch [mm]	Liquid crystal operation mode	Panel maker	Display manufacturer
1M (A)	1280×1024	0.312	IPS	NEC	Data-Ray (Precision 1)
(B)	1280×1024	0.281	IPS	ID-Tech	TOTOKU (ME181L)
2M (VA)	1600×1200	0.255	VA	SHARP	TOTOKU (ME201L)
(IPS)	1600×1200	0.270	IPS	NEC	TOTOKU (ME213L)
3M	2048×1536	0.207	IPS	ID-Tech	BARCO (MFGD3220)
5M (1)	2560×2048	0.165	IPS	ID-Tech	NANAO (RadiForceG51)
(2)	2560×2048	0.165	IPS	ID-Tech	TOTOKU (ME511L)
CRT (5M)	2560×2048	0.147	—	—	BARCO

the 1M LCDs, two kinds differing in the structure of pixels were used, and they were dubbed A and B, respectively. For the 2M display, two kinds also were used an in-plane switching (IPS) system and vertical alignment (VA) system[2], from which the liquid crystal operation mode differs.

The test pattern was displayed in the center of the screen, and a photograph was taken using a digital camera (Nikon D1H, D70) and camera equipped with a macro lens (Nikon AF Micro-Nikkor). Figure 2 shows the bar pattern image used as the test pattern. There were five pairs of bars with bar pattern and background luminance levels. Each bar consisted of a 1, 2, 3, 4 and 6-pixel width, respectively. The bar level was 65% of the digital driving level (DDL), and the background level was 35%.

The maximum luminance was set to 450 cd/m^2 and the minimum luminance to 1 cd/m^2. The displays were calibrated according to the DICOM 14 display function standard.[3] Therefore brightness of the bar level was about 98 cd/m^2, and those of the background level were about 21 cd/m^2.

1-2 Picturing the bar pattern

The measurement environment made the room dark, and luminance was about 0 lx. The bar pattern was displayed at the center of the display. Nothing was displayed in the surrounding area except for uniform the background with low DDL and some icons. Black paper covered the display surface except for the area of the bar pattern, to exclude the influence of illumination.

To lose the inclination to the image, the camera was placed parallel to the display.

We took pictures of a bar pattern in a horizontal direction and a vertical direction. We defined horizon-

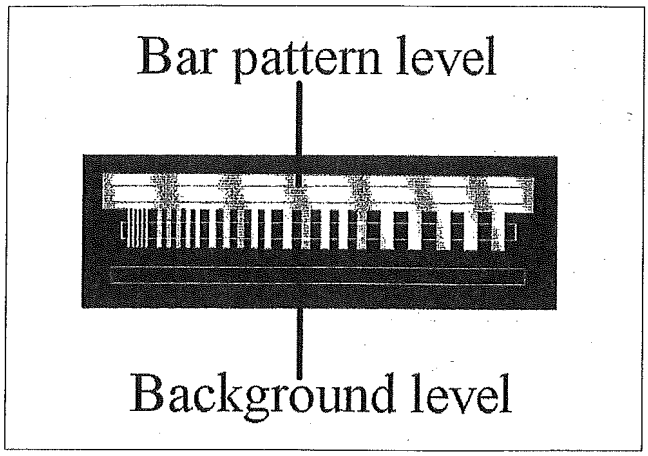

Fig. 2 Bar pattern image on display.

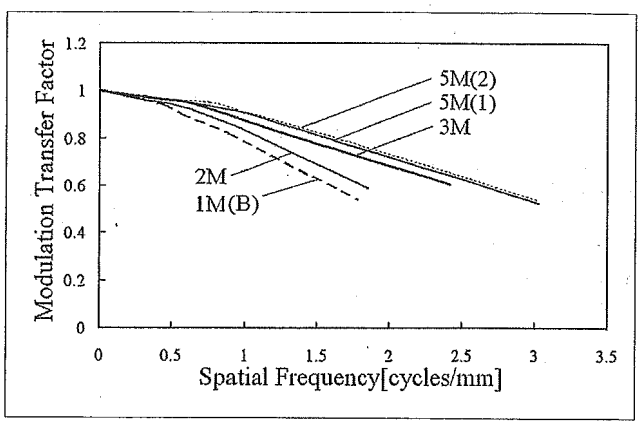

Fig. 3 MTFs in the horizontal direction of LCDs.

tal and vertical directions as portrait position and landscape position, respectively. When we took a picture of the bar pattern, the camera was not rotated, but the displays were rotated.

The distance between displays and the digital camera was adjusted so that a bar pattern would become the same size in the finder. Effective pixel number in the horizontal direction of the digital camera is 3040. We photographed the bar pattern image to become about 2000 pixels in the horizontal direction of the digital camera. At this time, the sampling pitch in the digital camera was 0.008–0.012 mm, and the sample number per one pixel of the display was 21–25.

The shutter speed of the camera was set to 1/5 second. Diaphragm was set to 29. The matrix size of the output image was 3040×2014, and its grayscale was 12 bit. We used RAW data from the CCD for calculation.

1-3 Calculation of MTFs

The data for exact integer cycles of the bar patterns were extracted from an output waveform. The amplitude value *Mn* of a fundamental frequency of bar pattern was calculated and MTF was computed.

2. Results

Figures 3 and 4 show MTFs of LCDs that have different numbers of pixels with the same structure of subpixels as an IPS system. The MTFs were measured to the Nyquist frequency decided from the pixel pitch of a display. MTFs in the horizontal direction are shown in Fig. 3, and those in the vertical direction are shown in Fig. 4. These MTFs were expressed with the spatial frequency corresponding to the real distance on the screen. In the horizontal direction, MTF of 5M was the highest, compared with those of 3M, 2M, and 1M. The two MTFs of 5M were almost the same. The MTFs of 1M and 2M were similar in the vertical direction. MTFs of 1M displays of the LCDs that differed in the structure of pixels are shown in Fig. 5. MTFs of 1M(A) exceeded 1 at low frequency. The fluctuation was also large, and their forms were different from other MTFs. MTFs of 2M displays of the LCDs with differences in liquid crystal operation mode are shown in Fig. 6. MTFs of the VA system in the horizontal and vertical directions were almost the same. MTFs of 5M displays of the LCD and CRT displays are shown in Fig. 7. MTFs of the CRT display decreased considerably compared with those of the LCD as frequency increased.

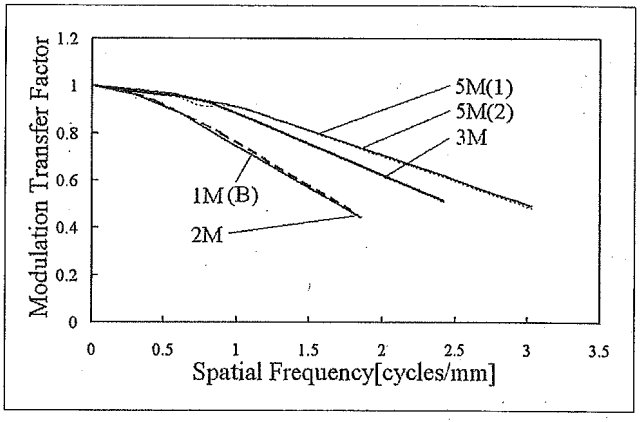

Fig. 4 MTFs in the vertical direction of LCDs.

3. Discussion

Enlarged images of pixels are shown in Fig. 8. We found that the shape of a pixel of 1M(A) was diamond-like and differed from other displays. Moreover, the width of a bar with one pixel was effectively narrower than

Eur Radiol (2006) 16: 726–732
DOI 10.1007/s00330-005-0030-3

H. Usami
M. Ikeda
T. Ishigaki
H. Fukushima
K. Shimamoto

The influence of liquid crystal display (LCD) monitors on observer performance for the detection of nodular lesions on chest radiographs

Received: 12 May 2005
Revised: 8 August 2005
Accepted: 13 September 2005
Published online: 12 November 2005

H. Usami (✉) · T. Ishigaki · H. Fukushima
Department of Radiology, Nagoya University Graduate School of Medicine, 65 Tsurumai-cho, Showa-ku, Nagoya, 466-8560, Japan
e-mail: hus-ygc@umin.ac.jp
Tel.: +81-52-7442328
Fax: +81-52-7442334

M. Ikeda · K. Shimamoto
Department of Radiological Technology, Nagoya University School of Health Sciences, 1-20 Daikominami 1-chome, Higashi-ku, Nagoya, 461-8673, Japan

Abstract *Purpose:* To access the influence of liquid crystal display (LCD) monitors on the detectability of nodular lesions depicted on chest radiographs by comparing them with a high-resolution cathode ray tube (CRT) monitor. *Material and methods:* Ten radiologists interpreted 247 soft-copy images on LCD monitors with pixel arrays of 1,024×1,280, 1,200×1,600, 1,536×2,048 and 2,048×2,560, and a CRT monitor with a pixel array of 2,048×2,560, and were asked to indicate their individual confidence levels regarding the presence of a nodule. These images were chest radiographs with and without a lung nodule from the "Standard Digital Image Database" created by the Japanese Society of Radiological Technology. The luminance distributions of all monitors were adjusted to the same, and the ambient illumination was 200 lux. Observer performance was analyzed in terms of the receiver-operating characteristics. *Results:* No significant statistical differences in nodule detection performance were found among the four LCD monitors and the CRT monitor. *Conclusion:* The nodule detection performance on the LCD monitors with a spatial resolution higher than a matrix size of 1,024×1,280 was found to be equivalent to that on the high-resolution CRT monitor.

Keywords Observer performance · Lung, nodule · Radiography, digital · Thorax, radiography · Lung, diagnosis

Introduction

Picture archiving and communication system (PACS) has currently come to play an important role in radiological practice [1]. Using PACS, radiologists make a diagnosis based on the images displayed on an electronic device, whereas, until a few years ago, cathode-ray-tube (CRT) monitors had been exclusively used as the display device.

A considerable number of studies [1–10] have been conducted to determine whether or not a CRT display monitor was an acceptable alternative to the traditional light box-viewing method of film images. Although a CRT monitor with an appropriate display performance (such as resolution, luminance range, gray scale, contrast, etc.) is now acceptable in place of the light box-viewing method [1–3, 5, 6, 9], a certain class of medical images viewed on a CRT monitor has not been accepted to date as an alternative to film images [4].

More recently, active-matrix liquid crystal display (LCD) monitors have been used as a display device for medical digital images [11–16], and LCD and CRT monitors are currently the two most common types used in diagnostic radiology systems [13–15]. LCD monitors have several advantages as well as disadvantages compared with CRT monitors [11, 13–15]. However, a few studies [17, 18] have so far been conducted on the performance of soft-copy reading using an LCD monitor, and little is known about the effects of LCD on the observer's performance.

Thus, the present study was carried out to evaluate the influence of LCD monitors with different display-pixel matrices on the detection performance of nodular lesions

depicted on chest radiographs by comparing them with a high-resolution CRT monitor.

Materials and methods

Observer-performance experiments were conducted to evaluate the effects of LCD monitors with different display-pixel matrices on the detectability of lung nodules on chest radiograph images.

Preparation of test images

For the image-reading experiment, we used the 247 posteroanterior chest radiograph images from the "Standard Digital Image Database" created by the Japanese Society of Radiological Technology [19]. The following brief description of the images in the "Standard Digital Image Database" is adapted from Ref. [19], consisting of 154 images with single nodules and 93 without nodules. Among the 154 images, 100 nodules were malignant and 54 were benign. The 154 images with single nodules were confirmed to include only one nodule per image, and the presence or absence of a single nodule was confirmed by CT examinations. The classification of malignant nodules was based on histological and cytological examinations, while the classification as benign was based either on histology, definitive isolation of a pathogenic organism, shrinkage and disappearance following the use of antibiotics or on no change observed during a follow-up period of 2 years. Among the 154 patients with nodules, 68 were male and 86 were female, and of the 93 without nodules, 51 were male and 42 were female. The size of the nodule was 5–10 mm for 31 patients, 11–15 mm for 52, 16–20 mm for 36, 21–25 mm for 14, 26–30 mm for 17 and 31–60 mm for 4, for an average size of 17.3 mm. The 154 single-nodule images were grouped into five category levels according to the degree of subtlety in detecting a lung nodule, based on the consensus of three chest radiologists. These category levels of subtlety were as follows: level 1, extremely subtle; level 2, very subtle; level 3, subtle; level 4, relatively obvious and level 5, obvious; 25 single-nodule images were categorized as level 1, 29 as level 2, 50 as level 3, 38 as level 4 and 12 as level 5. The images in the "Standard Digital Image Database" were so-called row-digital image data with a matrix size of 2,048×2,048 and a gray level of 12 bits, and were obtained by digitizing posteroanterior chest films using a film digitizer with a pixel size of 0.175 mm and an optical density range of 0.0–3.5. These image data were transformed into the DICOM image file format using our own program for display on the monitors and were stored on a compact disc.

LCD Monitors

In this study, we used four commercially available LCD monitors having different display-pixel matrices (their properties are listed in Table 1). As the comparative reference CRT, we used a high-resolution monochrome CRT monitor (BarcoView, Kortrijk, Belguim) with a maximum luminance of 600 cd/m^2 and a pixel array of 2,048×2,560 for a screen measuring 21 inches diagonally. We refer hereafter to these five types of monitors as by their abbreviated names shown in Table 1 (that is, 1M-LCD, 2M-LCD, 3M-LCD, 5M-LCD and CRT). These monitors were connected to PCs (personal computers) via a video board: the 1M-LCD monitor was connected by an MD2W video board (RealVision, Yokohama, Japan), the 2M-LCD by an LV22P2 (Totoku, Tokyo, Japan), the 3M-LCD by a 3MP2FH (BarcoView, Kortrijk, Belguim), the 5M-LCD by an MD5W (RealVision, Yokohama, Japan) and the CRT by an Md5PCX (DOME, USA). The 1M-LCD, 3M-LCD and CRT monitors had antireflective coatings. The test images prepared by the above-mentioned method were transferred to each of the PCs attached to the monitors via the compact disc.

For the sake of consistency in the image appearance on all five display monitors, we used the same software used

Table 1 Properties of LCD and CRT monitors used in observer-performance experiment

Abbreviations	Screen size (mm)	Pixel matrix	Maximum luminance (cd/m^2)	Manufacturer	Product name
1M-LCD	320×399	1,024×1,280 (SXGA)	700	Spectratech, Yokohama, Japan	Precision1M
2M-LCD	306×408	1,200×1,600 (UXGA)	700	Totoku, Tokyo, Japan	ME201L
3M-LCD	318×424	1,536×2,048 (QXGA)	700	BarcoView, Kortrijk, Belgium	MFGD3220D
5M-LCD	338×422	2,048×2,560 (QSXGA)	700	Eizo Nanao, Matto, Japan	G51
CRT	304×380	2,048×2,560 (QSXGA)	600	BarcoView, Kortrijk, Belgium	MDG521

for viewing the test images. The software for viewing medical images was designed for viewing on workstations (RS-252, Konica, Tokyo, Japan) and was installed in the PCs attached to all the monitors. Using this software, the images displayed were similar to the original film images on a light box. On all monitors, 12-bit digital image data were displayed by reducing the value of each 12-bit display pixel to 8-bits. On the 1M-LCD, 2M-LCD and 3M-LCD monitors, 2,048×2,048 digital image data were displayed by down sampling horizontal- and vertical-line data by the nearest-neighbor method.

The display functions of all five types of monitors were calibrated to the same by using the test pattern located in the central area with the uniform background, according to the recommendations of Digital Imaging and Communications in Medicine standard; the area of the test pattern was 10% of the whole display area of each monitor, and the luminance of the uniform background was 90 cd/m^2. Here, the maximum luminance was adjusted to 450 cd/m^2, and the minimum luminance was set at 1 cd/m^2. Maximum and minimum luminance values were set using the same ambient light conditions as those with which the reading process was conducted [16]. All five monitors were located side by side at similar heights from the floor (3M-LCD at a height of 75 cm, and the others at 82 cm). The study was conducted in the viewing workstation room at the Department of Radiology of the Nagoya University School of Medicine (Nagoya, Japan), thus ensuring that the light conditions were identical [16].

Image reading study

Ten radiologists (experience range, 8–22 years; mean experience, 15 years) agreed to participate in the observer performance studies. They were so-called general radiologists, none of whom were chest radiology specialists. For each observer, the image-reading test consisted of five sessions, in each of which each observer read all 247 images on one of the five types of monitors, so that each one saw the same 247 images on all five types.

Before beginning the test, the participants were informed of the following: 1) the test protocol; 2) there was one or no nodule in each image; 3) the ratio of the images of those with to those without single nodules was about 1.5:1; 4) the nodules were either benign or malignant. The observers were asked to estimate and report the probability of the presence of a single nodule (that is, to express a confidence level regarding its presence). Here, we used a continuous rating scale on a line-marking method to represent each observer's confidence level [20]. In this method, the observers were asked to mark their confidence level with a pencil on a line 10-cm long [20]. This line scale corresponded to a continuous rating ranging from 0 (left end of the scale) to 100 (right end of the scale) that represented the observer's confidence level regarding the presence of a nodule. A level of 0 or 100 corresponded to the definite absence or definite presence of nodules, respectively, while ratings between 0 and 100 indicated intermediate levels of confidence. Furthermore, observers whose confidence level was more than 0 were also asked to indicate on a rough sketch of a chest radiograph image the most suspicious position of the nodule they detected.

To average out learning effects, the 247 images were randomly displayed for each reader at each reading session. For each observer, the order of evaluation of monitor types in the five reading sessions was also varied randomly. No training session was held before each reading session. There was at least a 1-month interval between the reading sessions. During each session, no time constraints were imposed on any observer. The range and average of reading time were 33–162 min and 75 min, respectively. Although after seeing the images displayed together with a preset display function table, the observers were only allowed to use gray-level corrections (windowing) as the image processing functions during the reading sessions, very few elected to do so.

The ambient illumination was 200 lux during the viewing sessions, according to our previous study reported in Ref. [21].

Data analysis

The observers' detection performance was assessed using receiver-operating characteristic (ROC) analysis, in which a binormal ROC curve was fitted to each observer's confidence rating data from each reading session with a maximum-likelihood estimation. We used the Metz LABROC4 algorithm [22] to obtain maximum-likelihood estimates of binormal ROC curves from continuous ordinal-scale rating data. The area under the binormal ROC curve, A_z, was used as an index of observer performance. For summarizing ROC curves for each monitor type, average ROC curves were obtained by averaging the binormal slope and intercept parameters of the individual observer's ROC curves for each monitor.

Table 2 Analysis of Variance of Five Monitors for Areas under Binormal ROC Curves

Source*	Degree of freedom	Mean square	F ratio	Probability value
T	4	0.2471	0.8125	0.5255
R	9	3.4945	7.0511	0.0000
I	246	3.1179	6.2913	0.0000
T×R	36	0.3041	1.0229	0.4305
T×I	984	0.2927	0.9847	0.6280
R×I	2,214	0.4956	–	–
T×R×I	8,856	0.2973	–	–

*T=monitor types; I=images; R=readers

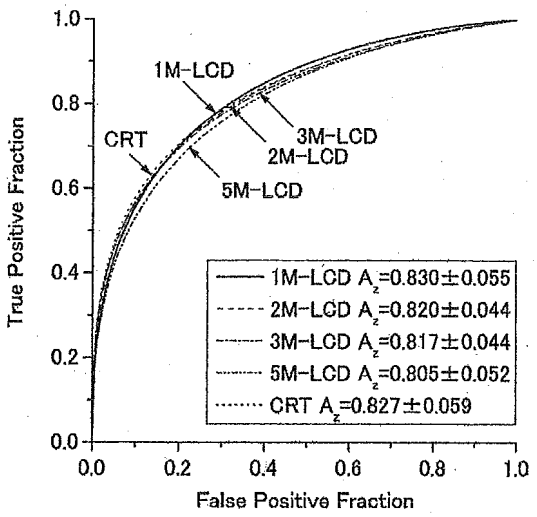

Fig. 1 Composite ROC curve for ten observers. Definitions of 1M-LCD, 2M-LCD, 3M-LCD, 5M-LCD and CRT are given in Table 1. A_z=estimated means of A_z±95% confidence intervals for each monitor type

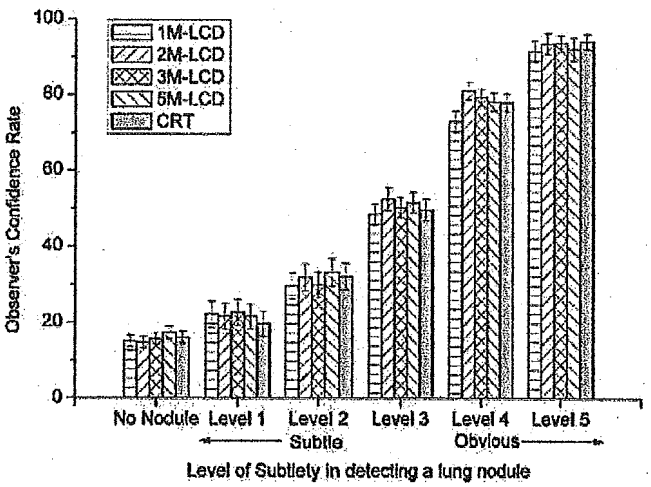

Fig. 2 Estimated means (±95% confidence intervals) of observer confidence rates regarding the presence of a nodule in images containing single nodules for each monitor type and for each degree of subtlety in detecting a nodule. The higher the level of subtlety in detecting a lung nodule, the easier the nodule detection; definitions of these subtlety levels are given in the text. For reference, the mean (±95% confidence intervals) of the observer confidence rates for images containing no nodule for each monitor type are also shown on the left

Our experimental design required a statistical analysis of the differences among the five types of monitors. We chose the analysis of variance (ANOVA) of pseudovalues of A_z computed by the jackknife-analysis method proposed by Dorfman et al. [23], and we designated it the Dorfman-Berbaum-Metz (DBM) method, based on Ref. [24].

Moreover, we also conducted ANOVA of the observer's confidence rates regarding the presence of a nodule in those images containing a nodule, with the monitor type and the degree of subtlety of the lung nodule as the fixed effect, and the observer as the random effect [25]. Pairwise comparisons among the means of the observer's confidence rates for the fixed effects were performed using Scheffé's multiple comparison tests or Tamhane's pairwise comparisons test [26], depending on the homogeneity of variance. We also conducted ANOVA of the observer's confidence rates for the presence of a nodule in those images containing no nodule, with the monitor type as the fixed effect and the observer as the random effect [25]. We used SPSS 12 software (SPSS Inc., Chicago, Ill.) for ANOVA.

We calculated the localization accuracy rate (P_{CL}), the ratio of all nodule images having nodules that were correctly indicated on a rough sketch by the observer, regardless of the confidence rates. We then estimated 95% confidence intervals by the maximum-likelihood method for the binomial model.

In our statistical analysis, a value of $P<0.05$ was accepted as significant.

Results

The observed differences in A_zs among the five monitor types were small. Results of the DBM ANOVA conducted on A_zs for the five monitor types are listed in Table 2. This overall ANOVA showed no statistically reliable effects of the five monitor types on the readers' diagnostic performances (P=0.5255). Statistically reliable differences in diagnostic performance were found among the ten observers ($P<0.001$) and among the 247 images ($P<0.001$). Figure 1 depicts the average ROC curves for the five monitor types, showing all five curves to be similar.

Table 3 Analysis of variance of five monitors for observer confidence rates for images with a single nodule

Source*	Degree of freedom	Mean square	F ratio	Probability value
T	4	1,733.424	1.130	0.3578
S	4	1,016,823.920	203.740	0.0000
R	9	32,334.931	6.153	0.0000
T×S	16	699.494	1.368	0.1655
T×R	36	1,533.888	2.819	0.0000
S×R	36	4,990.782	9.762	0.0000
T×S×R	144	511.223	0.725	0.9943

*T=monitor types; S=degrees of subtlety of lung nodules; R=readers

Table 4 Analysis of variance of five monitors for observer confidence rates for images with no nodule

Source*	Degree of freedom	Mean square	F ratio	Probability value
T	4	939.883	0.392	0.8133
R	9	44,129.229	18.383	0.0000
T×R	36	2,400.564	4.930	0.0000

*T=monitor types; R=readers

The overall ANOVA revealed that there were no statistically reliable differences in the observer confidence rates for images containing a single nodule among the five monitor types (P=0.3578), whereas there were statistically significant differences in them among the five degrees of subtlety in detecting lung nodules (P<0.001) and among the ten observers (P<0.001) (Table 3). Figure 2 shows that the differences in the estimated means of the observer confidence rates regarding the presence of a nodule for the images containing single nodules were also small among the five monitor types for each degree of subtlety in detecting a nodule. Due to the heterogeneity of variance, we conducted Tamhane's pairwise comparisons test [26] to reveal differences among mean observer confidence rates for any two levels of subtlety in a lung nodule, and our results showed statistically reliable differences among mean observer confidence rates between any two levels of subtlety of a lung nodule (P<0.001).

For the images containing no nodule, the overall ANOVA revealed that there were no statistically reliable differences in observer confidence rates among the five monitor types (P=0.8133), whereas there were statistically significant differences in those rates among the ten observers (P<0.001) (Table 4). Differences in the estimated means of observer confidence rates regarding the presence of a nodule for images containing no nodule were also small among the five monitor types (Fig. 2).

For some observers, there were statistically reliable differences in P_{CL} among the monitor types (Fig. 3). However, the relationship between the values of P_{CL} and the monitor types differed among the ten observers, and no general tendency in this relationship was recognized.

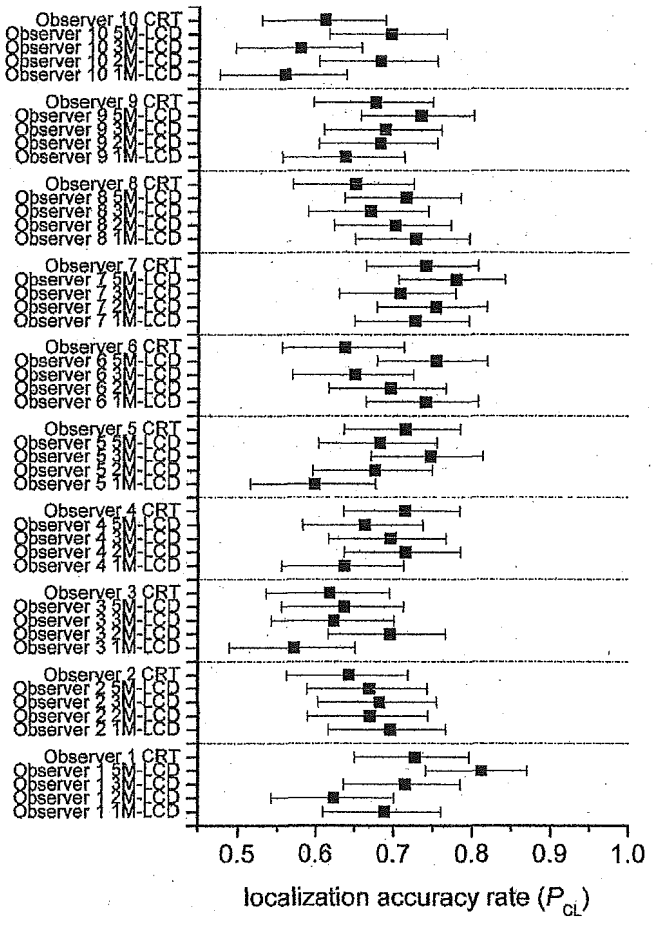

Fig. 3 Localization accuracy rates (P_{CL}'s) ± their 95% confidence intervals for each observer and for each monitor type. P_{CL} is the ratio of all nodule images having nodules that were correctly reported on a rough sketch by the observer regardless of the confidence rates. Their 95% confidence intervals were estimated by the maximum-likelihood method for the binomial model

Discussion

Our results indicate that there are no substantial differences in the nodule detection performance on chest radiographs among the five monitor types under the circumstances of this study. Thus, as far as the nodule detection performance on chest radiographs is concerned, the four types of LCD monitor used in this study are equivalent to the high-resolution CRT monitor, and no substantial differences are detectable among them. Under the appropriate display conditions, therefore, the nodule detection performance on the LCD monitor with a higher spatial resolution than a matrix size of 1,024×1,280 is equivalent to the one on the CRT monitor with a pixel array of 2,048×2,560. These results are compatible with those reported by Scharitzer et al. [16] and Kim et al. [12].

The most notable disadvantage of LCD monitors is their dramatic variations in luminance and contrast with the viewing angle [13, 15, 16]. In this study, since we gave the observers no special instructions about the viewing angle problem of LCD monitors, we believe that the effect of off-angle viewing was effectively eliminated by the correct viewing angle that the readers adopted spontaneously. Although the viewing angle problem may not have a highly detrimental effect on the detection performance of a nodule on chest radiographs, its effect on lesion detectability is still not well understood [15], and further studies are needed to resolve this problem.

Generally, the resolution properties of active-matrix LCDs are much better than those of CRTs, and the small-spot

contrast ratio of LCDs is higher (that is, better) than that of CRTs [15]. The characteristics of noise in LCDs are known to differ from those in CRTs [15]. At present, clinical performance cannot be predicted from physical parameters in chest radiography, and we must conduct observer performance study to evaluate it [27]. Under the conditions of the present study, when it comes to nodule detection on chest radiographs, the LCD monitor with a higher spatial resolution than a matrix size of 1,024×1,280 can be considered to convey almost the same information to the observer as the CRT monitor with a pixel array of 2,048×2,560, given the limitations of the observer's visual system.

This study indicates that, at least for nodule detection on chest radiographs, active-matrix LCD monitors with a higher spatial resolution than a matrix size of 1,024×1,280 are an acceptable alternative to CRT monitors with a pixel array of 2,048×2,560. CRT monitors with a pixel array of 2,048×2,560 may be accepted as an alternative to the traditional light box-viewing method for nodule detection [9]. Thus, active-matrix LCD monitors with a higher spatial resolution than a matrix size of 1,024×1,280 may also be an acceptable alternative to light box viewing for the nodule detection.

Here, as Scharitzer et al. pointed out in Ref. [16], it has to be noted that our results are valid only for the conditions under which the LCD monitors have the same relationship between luminance and pixel value as that in the reference CRT monitor. Of course, luminance range, gray scale and contrast, etc., should also be considered in addition to resolution when choosing an LCD monitor as a display system. However, most commercially available medical active-matrix LCD monitors are able to provide almost the same gradation characteristics as medical high-resolution CRT monitors.

The ambient illumination adopted in this study was rather high, compared with the standard one except in Japan. Under the other ambient illumination, the difference in the nodule detection performance among the five monitor types may alter. The effects of the ambient illumination deserve further consideration.

In the ANOVA performed on the observer's confidence rates for the presence of a nodule in the images containing a nodule and no nodule, there were significant interactions between the monitor type and reader. However, for each observer, the relationship between the estimated means of the observer's confidence rates and the monitor types showed no systemic relation between the observer's confidence rates and the resolution properties of monitors. So, we believe that these interactions will be due to a causal factor.

The levels of detectability of nodules in this study, including their degree of subtlety in detecting a lung nodule, were almost the same as those reported by Shiraishi et al. [19], and there was no inconsistency between the results of the present image reading experiment and theirs.

In conclusion, an LCD monitor with a higher spatial resolution than a matrix size of 1,024×1,280 can replace a high-resolution CRT monitor with a pixel array of 2,048×2,560 without any loss in the ability to detect pulmonary nodules on chest radiographs.

References

1. Iwano S, Ishigaki T, Shimamoto K et al (2001) Detection of subtle pulmonary disease on CR chest images: monochromatic CRT monitor vs color CRT monitor. Eur Radiol 11:59–64
2. Hertzberg BS, Kliewer MA, Paulson EK et al (1999) PACS in sonography: accuracy of interpretation using film compared with monitor display. Picture archiving and communication systems. Am J Roentgenol 173:1175–1179
3. Ishigaki T, Endo T, Ikeda M et al (1996) Subtle pulmonary disease: detection with computed radiography versus conventional chest radiography. Radiology 201:51–60
4. Wilson AJ (1995) Filmless musculoskeletal radiology: why is it taking so long? Am J Roentgenol 165:105–107
5. Razavi M, Sayre JW, Taira RK et al (1992) Receiver-operating-characteristic study of chest radiographs in children: digital hard-copy film vs 2K × 2K soft-copy images. Am J Roentgenol 158:443–448
6. Straub WH, Gur D, Good WF et al (1991) Primary CT diagnosis of abdominal masses in a PACS environment. Radiology 178:739–743
7. Slasky BS, Gur D, Good WF et al (1990) Receiver operating characteristic analysis of chest image interpretation with conventional, laser-printed, and high-resolution workstation images. Radiology 174:775–780
8. Foley WD, Jacobson DR, Taylor AJ et al (1990) Display of CT studies on a two-screen electronic workstation versus a film panel alternator: sensitivity and efficiency among radiologists. Radiology 174:769–773
9. Hayrapetian A, Aberle DR, Huang HK et al (1989) Comparison of 2,048-line digital display formats and conventional radiographs: an ROC study. Am J Roentgenol 152:1113–1118
10. Goodman LR, Foley WD, Wilson CR, Rimm AA, Lawson TL (1986) Digital and conventional chest images: observer performance with film digital radiography system. Radiology 158:27–33
11. Flynn MJ, Kanicki J, Badano A, Eyler WR (1999) High-fidelity electronic display of digital radiographs. RadioGraphics 19:1653–1669
12. Kim AY, Cho KS, Song KS, Kim JH, Kim JG, Ha HK (2001) Urinary calculi on computed radiography: comparison of observer performance with hard-copy versus soft-copy images on different viewer systems. Am J Roentgenol 177:331–335
13. Samei E, Seibert JA, Andriole K et al (2004) AAPM/RSNA Tutorial on equipment selection: PACS equipment overview: general guidelines for purchasing and acceptance testing of PACS equipment. RadioGraphics 24:313–334
14. Harisinghani MG, Blake MA, Saksena M et al (2004) Importance and effects of altered workplace ergonomics in modern radiology suites. RadioGraphics 24:615–627

15. Badano A (2004) AAPM/RSNA Tutorial on equipment selection: PACS equipment overview: display systems. RadioGraphics 24:879–889
16. Scharitzer M, Prokop M, Weber M, Fuchsjager M, Oschatz E, Schaefer-Prokop C (2005) Detectability of catheters on bedside chest radiographs: comparison between liquid crystal display and high-resolution cathode-ray tube monitors. Radiology 234: 611–616
17. Langer S, Bartholmai B, Fetterly K et al (2004) SCAR R&D Symposium 2003: comparing the efficacy of 5-MP CRT versus 3-MP LCD in the evaluation of interstitial lung disease. J Digit Imaging 17:149–157
18. Partan G, Mayrhofer R, Urban M, Wassipaul M, Pichler L, Hruby W (2003) Diagnostic performance of liquid crystal and cathode-ray-tube monitors in brain computed tomography. Eur Radiol 13:2397–2401
19. Shiraishi J, Katsuragawa S, Ikezoe J et al (2000) Development of a digital image database for chest radiographs with and without a lung nodule: receiver operating characteristic analysis of radiologists' detection of pulmonary nodules. Am J Roentgenol 174:71–74
20. Kobayashi T, Xu XW, MacMahon H, Metz CE, Doi K (1996) Effect of a computer-aided diagnosis scheme on radiologists' performance in detection of lung nodules on radiographs. Radiology 199:843–848
21. Itoh Y, Ishigaki T, Sakuma S et al (1992) Influence of CRT workstation on observer's performance. Comput Methods Programs Biomed 37: 253–258
22. Metz CE, Herman BA, Shen JH (1998) Maximum likelihood estimation of receiver operating characteristic (ROC) curves from continuously-distributed data. Stat Med 17:1033–1053
23. Dorfman DD, Berbaum KS, Metz CE (1992) Receiver operating characteristic rating analysis: generalization to the population of readers and patients with the jackknife method. Invest Radiol 27:723–731
24. Roe CA, Metz CE (1997) Dorfman-Berbaum-Metz method for statistical analysis of multireader, multimodality receiver operating characteristic data: validation with computer simulation. Acad Radiol 4:298–303
25. Tabachnick BG, Fidell LS (2001) Computer-assisted research design and analysis. Allyn and Bacon, Boston, UK
26. Hochberg Y, Tamhane AC (1987) Multiple comparison procedures. John Wiley & Sons, New York
27. Sund P, Båth M, Kheddache S, Månsson LG (2004) Comparison of visual grading analysis and determination of detective quantum efficiency for evaluating system performance in digital chest radiography. Eur Radiol 14:48–58